

Parameterization of Nonlinear Particle Resonances in Direct Laser Acceleration

F.-Y. Li, P. K. Singh, S. Palaniyappan, and C.-K. Huang*
Los Alamos National Laboratory, Los Alamos, New Mexico 87545, USA
(Dated: March 27, 2020)

Direct laser acceleration in plasmas is mainly ascribed to the resonances between the transverse electron oscillation and the laser oscillation. Here, we relax the usual paraxial limit and parameterize the nonlinear particle resonances based on the electron propagation angle. This approach allows the complete solution of the resonance momentum for any harmonic orders to be obtained for the first time. In particular, the solution shows direct correlation with electron's constant of motion, which permits general electron trapping conditions to be analyzed based on individual electron parameters. A wide parameter space spanned by the laser amplitude and the constant of motion is uncovered, which shows fine structures due to the complete resonances as well as the transition between the first- and high-order resonances. The elaborate parameter space built on the complete resonances will help optimize the acceleration and evaluate collective beam properties.

PACS numbers: 52.38.Kd, 52.38.-r, 52.57.-z, 41.60.Cr, 41.75.Jv

Laser acceleration of electrons widely exists in vacuum (whether open or bounded by dielectrics, magnets, or metals) [1], gases [2], and plasmas [3], etc. In a plasma, the acceleration normally happens when the radiation pressure associated with a picosecond intense pulse expels electrons, leaving a channel of much heavier ions. The resulting charge-separation field causes transverse electron oscillation or so-called betatron motion. When the betatron frequency coincides with the witnessed laser frequency, electrons start to see greatly more synchronized laser field oscillation. The direct laser acceleration (DLA) process, distinguished from the plasma-field acceleration [4], is thus initiated by the transverse laser electric field and quickly diverted forward by the magnetic field. The above acceleration due to betatron resonance [5] has been regarded as the leading mechanism of DLA. It is akin to the dynamics in a free-electron-laser (FEL) [6] or an inverse FEL accelerator [7], where magnetic wigglers play a similar role as the focusing plasma field. DLA has been found in a wide range of plasma densities [8–11], including overdense regimes where the laser channeling is enabled by either preformed plasma expansion [12] or relativistic transparency [13]. As such, DLA has been shown crucial to broad high-power laser applications such as electron fast ignition of inertial confinement fusion [14, 15], novel secondary source (X/ γ -ray, neutron, positron) production [10, 16, 17], and ion acceleration [18].

Many studies with Hamiltonian analysis [19, 20], test-particle tracking [21, 22], Monte-Carlo simulations [21], and particle-in-cell simulations [5, 23] have been reported on DLA. Despite these efforts, the involved nonlinear particle resonances have not been well parameterized. In fact, the role of betatron resonance is still being debated, for example, with recent proposals of a parametric instability due to nonlinear modulation of the betatron frequency [24] and a stochastic acceleration due to very high-order harmonic resonances [25]. Currently,

most theoretical modelings have been carried out in the limit of paraxial [22] or even axial condition [5]; whether non-paraxial solutions exist and what physical regimes do they point to are not clear. Even with the paraxial limit, a complete investigation into the resonance energy is still missing. The lack of these essential understandings has resulted in poor characterization of the laser-plasma and electron parameter space for electron trapping. As a consequence, low beam qualities, especially a substantial beam divergence, have been normally obtained from DLA experiments without much control [14, 26]. In this Letter, we present a systematic parameterization of the nonlinear particle resonances based on the electron propagation angle explicitly. This new approach leads to the first complete solution of the resonances, which breaks the usual paraxial limit and naturally covers the non-paraxial conditions for any harmonic orders. Based on that, we construct a framework that can treat the electron trapping over a wide parameter space in great detail. These new understandings of the resonances and the elaborate parameter space will benefit near-term experimental and theoretical studies on optimized beam generation from DLA as required for applications.

We present the central results based on a two-dimensional (2D) model of DLA, with the channel fields governed by a linear focusing electric field $E_{y,S} = k_e y$. Here, the field is normalized to $m_e \omega_0 c / e$, y to c / ω_0 , and $k_e = \omega_p^2 / 2\omega_0^2$ is proportional to the plasma density with ω_p being the plasma frequency and ω_0 the laser frequency. A plane-wave laser of electric field $E_{y,L} = a_0 \cos \phi$ and magnetic field $B_{z,L} = E_{y,L} / v_p$ propagates along $y = 0$, where a_0 is the normalized laser amplitude, v_p the phase velocity normalized to c , and $\phi = t - x / v_p$ the laser phase with t normalized to $1 / \omega_0$. The model can be extended to full electromagnetic [5] and 3D (e.g., Ref. [27]) with our key results unaffected. The electron dynamics follows the equations of motion $d\vec{p}/dt = -\vec{E} - \vec{v} \times \vec{B}$, $d\gamma/dt = -\vec{v} \cdot \vec{E}$, $d\vec{r}/dt = \vec{p} / \gamma$, with the kinetic mo-

mentum \vec{p} normalized to $m_e c$ and γ being the Lorentz factor. The nonlinear system has constants of motion $\gamma + U = C'_0$ when no laser is applied (i.e., inherent betatron motion), and $\gamma - p_x + U = C_0 + f(p_x)$ when the laser is switched on [5]. Here, $U = k_e y^2/2$ is the electrostatic potential, $C'_0 = \gamma_0 + U_0$ and $C_0 = \gamma_0 - v_p p_{x0} + U_0$ are related to initial electron parameters (p_{x0}, p_{y0}, y_0) with $\gamma_0 = \sqrt{1 + p_{x0}^2 + p_{y0}^2}$, $U_0 = k_e y_0^2/2$, and $f(p_x) = \epsilon p_x$ measures the effect of v_p with $\epsilon = v_p - 1 \ll 1$. For Gaussian lasers, the conservation law persists in the form albeit more complicated (e.g., Ref. [21]). A salient feature of DLA is normally found in the betatron amplitude, y_m , which readily approaches the asymptotic boundary $y_b = \sqrt{2C_0/k_e}$ (assuming $\epsilon = 0$). From the constant of motion, this happens when $\gamma - p_x$ sufficiently approaches zero at $p_y = 0$ mainly due to electron acceleration. Notice that in vacuum (i.e., $k_e = 0$), $\gamma - p_x$ is basically a constant and no net acceleration occurs [28]. Motivated by the simplified betatron motion $y = h y_b \cos \theta$, we transform the motion equations into

$$\frac{d\gamma}{d\theta} = a_0 h y_b \sin \theta \cos \phi + C_0 h^2 \sin 2\theta, \quad (1a)$$

$$\frac{d\phi}{d\theta} = \frac{C_0(2 - h^2 - h^2 \cos 2\theta)}{\sqrt{k_e \gamma}}, \quad (1b)$$

where θ is the betatron phase and h is usually close to unity in the course of DLA. It is seen that the laser work, $W_L = \int a_0 h y_b \sin \theta \cos \phi d\theta$, highly depends on the beating of the laser phase with the betatron phase which can be non-trivial. The calculation is greatly simplified by considering a strong inherent betatron motion (i.e., $p_{y0} > 0$ and $\gamma_0 \gg 1$), which we shall see is normally required for the high-harmonic resonances. Perturbing from that (see the Supplementary Material), we can arrive at $\phi = l\theta + d_1 \sin 2\theta + \phi''$, where l , d_1 and ϕ'' are constants related to initial laser-plasma and electron conditions, and they satisfy $l \gg d_1$. Plugging it into W_L , we find that for the integral to be pronounced over a few betatron cycles, the choices of l are narrowed down around odd integers. This result suggests that odd-harmonic resonances are more effective over longer interactions. Therefore, the required frequency-matching is obtained as $d\phi/dt = ld\theta/dt$ by neglecting the small term due to d_1 . Making use of the betatron frequency $\omega_\beta = d\theta/dt = \sqrt{k_e/\gamma}$ and the witnessed laser frequency $\omega_d = d\phi/dt = 1 - p_x/\gamma v_p$, we recast it as

$$l\sqrt{k_e \gamma} = \gamma - p_x + \chi f(p_x), \quad (2)$$

where l can be conceived as the harmonic order and $\chi = 1/v_p$. As we have seen, this matching relation should be inherently averaged over θ if l reduces to integers. Alternatively, since $\gamma - p_x$ is linked to y by the constant of motion, the averaging of Eq. (2) is straightforward given that y takes the sinusoidal form.

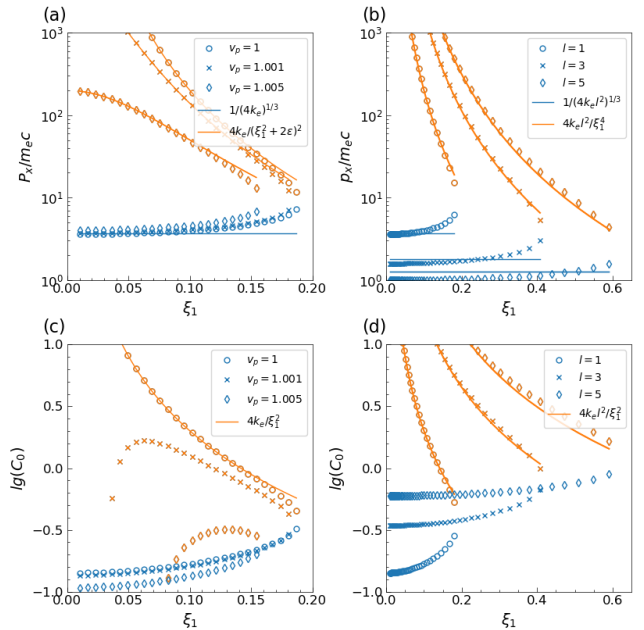


FIG. 1: Complete solution of the nonlinear resonances. (a) Resonance p_x versus ξ_1 for the first-order resonance $l = 1$ and different laser phase velocities v_p and (b) for $v_p = 1$ and different l . (c) and (d) Constant of motion C_0 versus ξ_1 at corresponding conditions of (a) and (b). The blue and orange colors represent the low and high branches, respectively. The solid lines refer to Eq. (4) in (a) and (b) and Eq. (6) in (c) and (d). In the calculations we take $\omega_p/\omega_0 = 0.1$.

To solve for the resonance momentum, we cast $\gamma = p_x \sqrt{1 + \xi_1^2 + \xi_2^2}$ where $\xi_1 = p_y/p_x$ and $\xi_2 = 1/p_x$. Notice that $\xi_1 \equiv \sqrt{\langle \xi_1^2 \rangle}$ due to its dynamic signs, where $\langle \dots \rangle$ stands for averaging over θ and is omitted throughout for simplicity. Instead of approximating ξ_1 and ξ_2 for various limits [5, 22], here we retain both and crucially treat ξ_1 as a free parameter. This simple approach allows to obtain complete solutions and also identify their correlation with ξ_1 . Physically, ξ_1 measures the electron propagation angle or the betatron strength (akin to the K -parameter in FELs [6]), and it also contains key information about the divergence when applied to a beam of electrons. With this form of γ , Eq. (2) can be arranged in terms of ξ_2 , or p_x , as $(1 - k_e^2 l^4) \xi_2^4 - 4k_e \chi l^2 \xi_2^3 + [(2 - l^4 k_e^2)(1 + \xi_1^2) - 2\chi^2] \xi_2^2 - 4k_e \chi l^2 (1 + \xi_1^2) \xi_2 + [\xi_1^4 + (1 - \chi^2)(1 - \chi^2 + 2\xi_1^2)] = 0$. This polynomial equation is found to give a pair of real roots for a reasonable range of k_e , v_p and ξ_1 , corresponding to two distinct branches of resonance. Figures 1(a) and 1(b) show the solution in p_x for different v_p and l . It is seen that the two branches vary differently against ξ_1 , and they become degenerated at a cut-off, ξ_1^{cut} , beyond which the solution is prohibited. Under the paraxial limit (i.e., with $\xi_1^2 \ll 1$), we can also extract from Eq. (2) simple scaling relations with ξ_1 as

$$p_x = k_e v_p^2 l^2 \frac{1 - (\xi_1^2 + \xi_2^2)/4}{[(\xi_1^2 + \xi_2^2)/2 + \epsilon]^2}. \quad (3)$$

The scaling can be further simplified in the limit of (1) $v_p = 1$, $\xi_1 = 0$ and (2) $\xi_1 \gg \xi_2$ as

$$p_x^{(1)} = \frac{1}{(4k_e l^2)^{1/3}}, \quad p_x^{(2)} = \frac{4k_e l^2}{(\xi_1^2 + 2\epsilon)^2}. \quad (4)$$

As presented by the solid curves in Figs. 1(a) and 1(b), they correspond to the low- and high-momentum branches, respectively. By comparing with the seminal work [5], it is now clear that only the limit of $\xi_1 = 0$ was considered in the latter; this axial condition led to the finding of only the low branch of $p_x^{(1)}$ for the luminal condition ($\epsilon = 0$), with the high branch being infinitely large and becoming lowered only when $\epsilon > 0$. However, the limit of $\xi_1 = 0$ corresponds to vanished betatron motion and should not be of practical interest for DLA. Here, we show for the first time that there actually exists a whole range of ξ_1 that can accommodate both the two branches simultaneously for arbitrary v_p and harmonic orders. For $\xi_1 > 0$, while the low branch is only slightly increased from $p_x^{(1)}$, the corresponding high branch, $\propto 1/\xi_1^4$, is brought down rapidly to accessible levels. The cut-off, $\xi_1^{\text{cut}} \simeq (4k_e l^2)^{1/3}$, can thus be estimated by letting $p_x^{(2)} = p_x^{(1)}$. This result importantly suggests that the paraxial condition only applies to low plasma densities and low harmonic orders. While at high densities or high orders, the allowed range of ξ_1 can be significantly extended and eventually fall into the non-paraxial condition, where the polynomial equation is required to find the solutions. Another feature of the non-paraxial condition occurs for the low-branch momentum, which may reduce to negligible levels following $p_x^{(1)} = 1/\xi_1^{\text{cut}}$. This trend is clearly seen in Fig. 1(b) by the solution for $l = 5$, where the high branch starts to dominate the full momentum range.

Given the broad range of the allowed ξ_1 , an important question next is about the accessibility to a particular ξ_1 for a given electron. Since the constant of motion has connections to initial electron conditions, we consider averaging of it near the onset of resonance. The associated betatron amplitude can be obtained as $y_m = \sqrt{1 + f(\tilde{p}_x)/C_0 - g(\tilde{p}_x)/C_0 y_b}$, where $g(\tilde{p}_x) = \sqrt{1 + \tilde{p}_x^2} - \tilde{p}_x$ and \tilde{p}_x denotes the value of p_x when $p_y = 0$ or $y = y_m$. The factor g may not be ignored for the low branch when $\tilde{p}_x \sim \mathcal{O}(1)$, so is f for the high branch when ϵ is large. Nevertheless, their impact on the variation of y_m tends to be minimized due to the nonlinear dependence of y_m on \tilde{p}_x . Assume y_m varies little over the course, then averaging of the constant of motion over θ gives

$$C_0(\xi_1, p_x) = 2p_x(\sqrt{1 + \xi_1^2 + \xi_2^2} - 1) - f(p_x) - g(p_x), \quad (5)$$

where we no longer distinguish \tilde{p}_x from the averaged p_x since they are differed slightly and the difference is further minimized through f and g . Equation (5) crucially links particular resonance quantities ξ_1 and p_x to the initial electron conditions by the constant of motion C_0 . It

is worth noting that in Ref. [22], ξ_2 was dropped due to the paraxial approximation, so that only the high branch was found for $\epsilon = 0$ by averaging over $y_m = y_b$ which was only good for large p_x . By substituting the solution of $p_x(\xi_1)$ from Eq. (2), we transform Eq. (5) into $C_0(\xi_1)$ with single dependence on ξ_1 for the two branches, as presented in Figs. 1(c) and 1(d). When $v_p > 1$, the effective space of C_0 contracts as ϵ increases, implying more constraints on the accessibility under superluminal conditions. While under the luminal condition, C_0 can extend to the full range, where the high branch typically has $C_0 > 1$ with the electron parameters dominated by large (p_{y0}, y_0) , and the low branch has $C_0 < 1$ with p_{x0} being the dominant one. By using $p_x^{(2)}$ from Eq. (4), the high branch under the paraxial and luminal conditions has simple relations

$$C_0 = \frac{4k_e l^2}{\xi_1^2}, p_x = \frac{C_0^2}{4k_e l^2}, \Delta p_x|_{l+2} = \frac{C_0^2}{k_e} \frac{l+1}{l^2(l+2)^2}, \quad (6)$$

where the mapping between p_x and C_0 is obtained by cancelling out their dependence with ξ_1 . The resulting p_x shows discrete levels given that only integers are considered for l as required for effective DLA. These quantum-like momentum transitions have been observed at very high-order resonances as a stochastic effect [25]. Here, with our new framework built on the complete resonances, we are able to clarify such a phenomenon in great detail. As illustrated by Fig. 1(d), electrons starting from a given C_0 can be in resonance at different harmonic orders with different ξ_1 . As a result, the transitions in p_x also lead to jumps in ξ_1 , which under the paraxial limit follows $\xi_1 = \sqrt{4k_e l^2/C_0}$. The momentum gap between each successive levels, $\Delta p_x|_{l+2}$, remains small at large l , indicating easy transitions at very high-order resonances. However, when $l \rightarrow 1$ the transition may be eventually suppressed due to the substantially increased gaps.

The above framework permits to find general electron trapping conditions. The onset of DLA essentially relies on small electron dephasing relative to the laser. According to Eq. (1b), we find that the averaged dephasing is $\langle d\phi/d\theta \rangle = l$, which is proportionally larger with the harmonic order. Given that $h \simeq 1$, the minimum dephasing $d\phi/d\theta \simeq 0$ is only briefly reached when y hits boundaries (i.e., $\theta = N\pi$ with N being integers). Thus, as l increases, the domain in θ for small dephasing quickly converges towards $\theta = N\pi$, where the momentum transition happens [25]. High-harmonic orders normally correspond to large C_0 as $l \sim C_0/2\sqrt{k_e \gamma}$. The associated strong inherent betatron motion thus results in $h \simeq 1$, which can naturally trigger off DLA around $\theta = N\pi$. However, this behaviour is absent for the first-order resonance, where the dephasing is overall small and electrons see almost continuous energy exchange. As such, the first-order resonance has to be invoked by a strong acceleration near its onset, i.e., $\Delta p_x \sim v_y a_0 \Delta t \geq p_x - p_{x0}$, where p_x is the corresponding resonance momentum. In terms of the

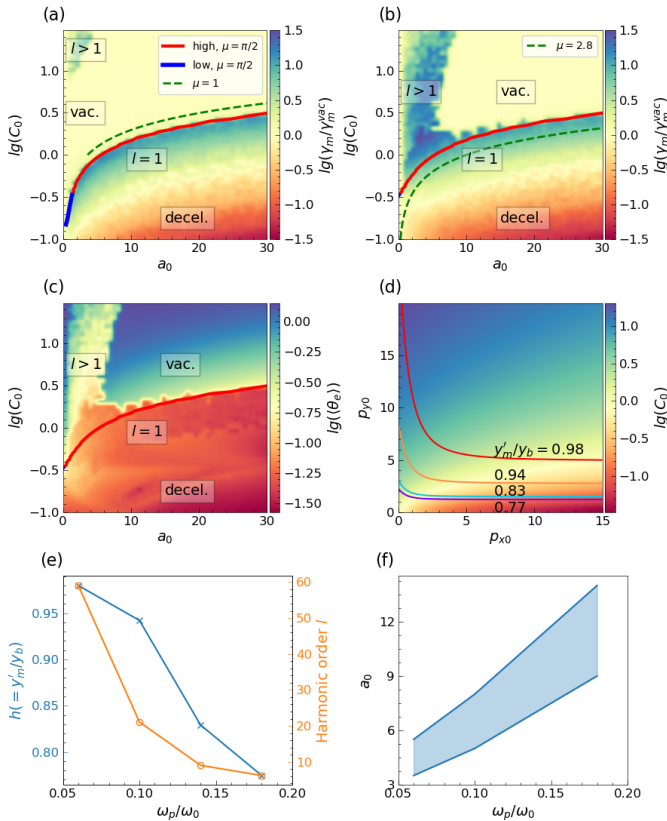


FIG. 2: The parameter space spanned by laser amplitude a_0 and constant of motion C_0 covering both the low- and high-branches and both the first- and high-order resonances. (a) Energy gain ratio $\gamma_m/\gamma_m^{\text{vac}}$ for the cases $p_{xa} = p_{ya} = 0$ and (b) $p_{xa} = p_{ya} = 2$, where $\omega_p/\omega_0 = 0.1$ is taken. (c) Averaged electron propagation angle $\langle \theta_e \rangle$ corresponding to case (b). (d) Distribution of C_0 in terms of (p_{x0}, p_{y0}) with the contours showing the ratio y'_m/y_b at different levels. (e) The threshold h required to trigger off high-order resonances when $p_{x0} = 0$ and corresponding harmonic order l at different ω_p/ω_0 . (f) The boundary in a_0 for the high-order resonances with the shaded area indicating the variations at different C_0 .

resonance quantities, i.e., $v_y \sim \xi_1$, $\Delta t \sim \omega_\beta^{-1} \sim \sqrt{p_x/k_e}$, this requirement can be cast into a threshold for a_0 ,

$$a_0^{\text{th}}(C_0, p_{x0}) = \frac{\mu}{\sqrt{2}} \frac{p_x - p_{x0}}{\sqrt{p_x} \xi_1} \frac{\omega_p}{\omega_0}, \quad (7)$$

where μ is a scaling constant, and $p_x(C_0)$ and $\xi_1(C_0)$ can be supplied by our complete solution of the resonances. By including p_{x0} , our approach allows to investigate the effect of individual electron parameters, rather than just that of the constant of motion C_0 [22, 25]. It is particularly important for the low branch having $p_x \sim \mathcal{O}(p_{x0})$. It is also important for the high branch when p_{x0} is large, for example, with injections from pre-acceleration.

To verify these findings, we perform numerical simulations by solving the original equations of motion in time. A wide parameter space spanned by a_0 and C_0 is investigated, where we take $v_p = 1$ and $y_0 = 0$ for simplic-

ity. The free choice in (p_{x0}, p_{y0}) is assessed by including a pair of constants (p_{xa}, p_{ya}) for a given distribution of C_0 , i.e., $p_{x0} = \frac{1+p_{ya}^2-C_0^2}{2C_0}$, $p_{y0} = p_{ya}$ for $C_0 \leq 1$ and otherwise, $p_{x0} = p_{xa}$, $p_{y0} = \sqrt{C_0^2 - 1 + 2p_{xa}C_0}$. Figures 2(a) and 2(b) first present the energy gain ratio of $\gamma_m/\gamma_m^{\text{vac}}$ (i.e., the ratio of maximum energy to that achievable in vacuum [28]) for the cases $p_{xa} = p_{ya} = 0$ and $p_{xa} = p_{ya} = 2$, respectively. Although both cases have the same C_0 distribution, they give very different patterns in the energy gain via DLA. This clearly demonstrates the inadequacy of using just C_0 to describe the parameter space. Typically, the space is divided into first- and high-order resonances, with also deceleration ($\gamma_m/\gamma_m^{\text{vac}} < 1$) and vacuum-like ($\gamma_m/\gamma_m^{\text{vac}} \simeq 1$) dynamics identified. The onset of the first-order resonance is well described by Eq. (7) with $\mu = \pi/2$ as seen by the solid lines. For the case $p_{xa} = p_{ya} = 0$, it particularly shows a segment (blue color) at small C_0 dedicated to the low-branch resonance. While for the case $p_{xa} = p_{ya} = 2$, the contribution due to the low branch is greatly reduced because p_{x0} at small C_0 is now significantly increased, even above the low-branch momentum. Notice that, Eq. (7) simplifies to $a_0^{\text{th}} = \frac{\mu}{2\sqrt{2}} \left(\frac{\omega_0}{\omega_p}\right) C_0^{3/2}$ for the high branch by assuming $p_x \gg p_{x0}$. This is the scaling obtained in Ref. [22] with $\mu = 1$. Nevertheless, they obtained the scaling for $p_{x0} = 0$, thus only applicable to $C_0 \geq 1$ as displayed by the dashed line in Fig. 2(a). Figure 2(c) also presents the distribution of averaged electron propagation angle corresponding to the case of Fig. 2(b). It is seen that the onset of DLA typically results in much smaller angles than in the vacuum-like dynamics. The angles also increase with harmonic orders, implying the transition to non-paraxial conditions, which is consistent with Fig. (1). These observations may suggest that small beam divergence can be realized in DLA by controlling more electrons to enter the first-order resonance.

The high-order resonances show strong dependence on individual electron parameters. As seen in Fig. 2(b), significantly enlarged region for $l > 1$ is found when choosing $p_{xa} = p_{ya} = 2$. The onset condition of very high-order resonances was given by $\mu \ll 2.8$ in Ref. [25], as seen by the area above the dashed line. However, we uncover a vast area of vacuum-like dynamics in transition between the high- and first-order resonances. The high-order resonances are bordered by two boundaries in C_0 and a_0 , respectively. The boundary in C_0 is clearly visible in Fig. 2(a) where p_{x0} is kept zero for $C_0 > 1$. To account for that, we consider the maximum amplitude for the incoherent betatron motion which is $y'_m = \sqrt{\frac{2(\gamma_0 - \sqrt{1+p_{x0}^2})}{k_e}}$ assuming $y_0 = 0$. Its ratio to y_b under small a_0 (i.e., $p_x \sim p_{x0}$ when $p_y = 0$) is $y'_m/y_b = \sqrt{\frac{\gamma_0 - \sqrt{1+p_{x0}^2}}{\gamma_0 - p_{x0}}}$. This ratio is plotted in Figs. 2(d) for different (p_{x0}, p_{y0}) . It is seen that when $p_{x0} = 0$, large p_{y0} is required to trigger

off the high-order resonances by having $y'_m/y_b = h \rightarrow 1$. This corresponds to a threshold in C_0 which is reduced to $C_0 = \sqrt{1 + p_{y0}^2}$. It is also seen that the required p_{y0} or C_0 quickly declines as finite p_{x0} is involved. This explains in Figs. 2(b) with $p_{x0} = 2$ why the boundary in C_0 already connects with that for the first-order resonance. The boundary in C_0 also has dependence on ω_p/ω_0 (or plasma density). At high densities, the required $h = y'_m/y_b$ to trigger off DLA can be reduced as presented in Fig. 2(e). This result is obtained by solving Eq. (1) for different C_0 with $h = \sqrt{1 - 1/C_0}$ which is the case for $p_{x0} = 0$. The lowered requirement on h is because of the reduced harmonic order $l \sim \sqrt{C_0/2k_e}$ at correspondingly larger k_e , implying transition to the first-order-type DLA. The boundary in a_0 is more complicated. While DLA can be triggered off with small a_0 at very high-order resonances, it becomes suppressed at large enough a_0 . Physically, accessing the last few low orders would need to overcome large momentum gaps as given by Eq. (6). This requires large a_0 , which however tends to transform the electron dynamics into vacuum-like with $h \rightarrow 0$. A parameter scan shows that the threshold a_0 scales proportionally with plasma density as seen in Fig. 2(f). The upper and low limits of the shaded area correspond to the boundaries at large and small C_0 , respectively. This trend is because larger a_0 is needed to overcome stronger inherent betatron motion which has larger C_0 .

The parameter space as elaborated in Fig. 2 will be useful to the control of DLA by optimizing laser-plasma parameters for potential electron injections. For example, when the electrons are dominated by large C_0 with large transverse energies, the high-order resonances may be more relevant since the first-order resonance typically demands very strong lasers to be switched on; while for electrons having small C_0 , a proper choice of laser amplitude would allow most of the electrons to enter the first-order resonance which may give optimized beam collimation. Obviously, the dependence of the parameter space on individual (p_{x0}, p_{y0}) as we have emphasized in this work will be crucial to the precision of the above control.

In summary, we have obtained the first complete solution of the nonlinear particle resonances in DLA. It is achieved by treating the electron propagation angle as a free parameter. This simple approach is used to clarify the various limits found in the literature, and treat both the paraxial and non-paraxial conditions self-consistently for any harmonic-resonance orders. Built on the complete solution, we have further constructed a framework that can analyze electron trapping for a wide parameter space based on individual electron parameters. It is hoped that this capability will stimulate near-term experiments with better control. The explicit inclusion of electron angle in our modeling may also help evaluate the divergence for a beam of electrons, a key property of DLA that needs to be optimized for many applications.

F.Y.L. and C.K.H. thank Joshua Burby, Nathan Garland, and Xianzhu Tang for helpful discussions. The work is supported by the Laboratory Directed Research and Development Program of Los Alamos National Laboratory (LANL) under the project 20190124ER. Computations are supported by the Institution Computing Program at LANL.

* huangck@lanl.gov

- [1] R. J. England, R. J. Noble, K. Bane, D. H. Dowell, C.-K. Ng, J. E. Spencer, S. Tantawi, Z. Wu, R. L. Byer, E. Peralta, et al., *Reviews of Modern Physics* **86**, 1337 (2014).
- [2] W. Kimura, G. Kim, R. Romea, L. Steinhauer, I. Pogorelsky, K. Kusche, R. Fernow, X. Wang, and Y. Liu, *Physical review letters* **74**, 546 (1995).
- [3] J. Meyer-ter Vehn and Z. M. Sheng, *Physics of Plasmas* **6**, 641 (1999).
- [4] T. Tajima and J. M. Dawson, *Physical Review Letters* **43**, 267 (1979).
- [5] A. Pukhov, Z.-M. Sheng, and J. Meyer-ter Vehn, *Physics of Plasmas* **6**, 2847 (1999).
- [6] Z. Huang and K.-J. Kim, *Physical Review Special Topics-Accelerators and Beams* **10**, 034801 (2007).
- [7] E. Courant, C. Pellegrini, and W. Zakowicz, *Physical review. A* **32**, 2813 (1985).
- [8] C. Gahn, G. Tsakiris, A. Pukhov, J. Meyer-ter Vehn, G. Pretzler, P. Thirolf, D. Habs, and K. Witte, *Physical Review Letters* **83**, 4772 (1999).
- [9] G. Malka, M. Aleanard, J. Chemin, G. Claverie, M. Harston, J. Scheurer, V. Tikhonchuk, S. Fritzler, V. Malka, P. Balcou, et al., *Physical review E* **66**, 066402 (2002).
- [10] H. Chen, F. Fiuza, A. Link, A. Hazi, M. Hill, D. Hoarty, S. James, S. Kerr, D. Meyerhofer, J. Myatt, et al., *Physical review letters* **114**, 215001 (2015).
- [11] I. Tsymbalov, D. Gorlova, S. Shulyapov, V. Prokudin, A. Zavorotny, K. Ivanov, R. Volkov, V. Bychenkov, V. Nedorezov, A. Paskhalov, et al., *Plasma Physics and Controlled Fusion* **61**, 075016 (2019).
- [12] A. Krygier, D. Schumacher, and R. Freeman, *Physics of Plasmas* **21**, 023112 (2014).
- [13] S. Palaniyappan, B. M. Hegelich, H.-C. Wu, D. Jung, D. C. Gautier, L. Yin, B. J. Albright, R. P. Johnson, T. Shimada, S. Letzring, et al., *Nature Physics* **8**, 763 (2012).
- [14] L. Jarrott, M. Wei, C. McGuffey, A. Solodov, W. Theobald, B. Qiao, C. Stoeckl, R. Betti, H. Chen, J. Delettrez, et al., *Nature Physics* **12**, 499 (2016).
- [15] T. Gong, H. Habara, K. Sumioka, M. Yoshimoto, Y. Hayashi, S. Kawazu, T. Otsuki, T. Matsumoto, T. Minami, K. Abe, et al., *Nature communications* **10**, 1 (2019).
- [16] S. Cipiccia, M. R. Islam, B. Ersfeld, R. P. Shanks, E. Brunetti, G. Vieux, X. Yang, R. C. Issac, S. M. Wiggins, G. H. Welsh, et al., *Nature Physics* **7**, 867 (2011).
- [17] J. C. Fernández, D. Cort Gautier, C. Huang, S. Palaniyappan, B. J. Albright, W. Bang, G. Dyer, A. Favalli, J. F. Hunter, J. Mendez, et al., *Physics of*

- plasmas **24**, 056702 (2017).
- [18] J. Bin, M. Yeung, Z. Gong, H. Wang, C. Kreuzer, M. Zhou, M. Streeter, P. Foster, S. Cousens, B. Dromey, et al., *Physical review letters* **120**, 074801 (2018).
- [19] J. Angus and S. Krasheninnikov, *Physics of Plasmas* **16**, 113103 (2009).
- [20] Y. Zhang and S. Krasheninnikov, *Physics of Plasmas* **25**, 013120 (2018).
- [21] G. Tsakiris, C. Gahn, and V. Tripathi, *Physics of Plasmas* **7**, 3017 (2000).
- [22] V. Khudik, A. Arefiev, X. Zhang, and G. Shvets, *Physics of Plasmas* **23**, 103108 (2016).
- [23] B. Liu, H. Wang, J. Liu, L. Fu, Y. Xu, X. Yan, and X. He, *Physical review letters* **110**, 045002 (2013).
- [24] A. V. Arefiev, B. N. Breizman, M. Schollmeier, and V. N. Khudik, *Physical review letters* **108**, 145004 (2012).
- [25] Y. Zhang, S. Krasheninnikov, and A. Knyazev, *Physics of Plasmas* **25**, 123110 (2018).
- [26] C. Gahn, G. Tsakiris, G. Pretzler, K. Witte, P. Thirolf, D. Habs, C. Delfin, and C.-G. Wahlström, *Physics of plasmas* **9**, 987 (2002).
- [27] T. W. Huang, C. T. Zhou, A. P. L. Robinson, B. Qiao, A. V. Arefiev, P. A. Norreys, X. T. He, and S. C. Ruan, *Physics of Plasmas* **24**, 043105 (2017).
- [28] J. Meyer-ter Vehn, A. Pukhov, and Z.-M. Sheng, in *Atoms, Solids, and Plasmas in Super-Intense Laser Fields* (Springer, 2001), pp. 167–192.